Magnetic and magnetostrictive properties in amorphous $(Tb_{0.27}Dy_{0.73})(Fe_{1-x}Co_x)_2$ films



2000 J. Phys.: Condens. Matter 12 7957

(http://iopscience.iop.org/0953-8984/12/36/310)

J. Phys.: Condens. Matter **12** (2000) 7957–7968. Printed in the UK PII: S0953-8984(00)10730-1

# Magnetic and magnetostrictive properties in amorphous $(Tb_{0.27}Dy_{0.73})(Fe_{1-x}Co_x)_2$ films

N H Duc†, K Mackay, J Betz, Zs Sárközi‡ and D Givord

Laboratoire Louis Néel, CNRS, BP-166, 38042 Grenoble Cédex 9, France

E-mail: sarkozi@phys.ubbcluj.ro

Received 4 January 2000, in final form 13 June 2000

**Abstract.** Magnetic and magnetostrictive properties have been investigated for amorphous $(Tb_{0.27}Dy_{0.73})(Fe_xCo_{1-x})_2$ thin films. An increase in the 3d magnetic moment and Curie temperatures higher than 550 K due to the enhancement of T–T interactions (T = transition metal) in substituted (Fe, Co) alloys were found. A well defined in-plane anisotropy is created by magnetic field annealing for the Co-rich films. A large magnetostriction of $480 \times 10^{-6}$ was developed in 1.8 T magnetic field and $350 \times 10^{-6}$ in low fields of 0.06 T for films with $x = 0.47$ after magnetic field annealing. The differing roles of Fe and Co atoms in the magnetization process have also been investigated.

## 1. Introduction

Over the past few years there has been a growing interest in magnetic thin films with large magnetostriction [1–3]. This interest is motivated by the potential such films show for use in microsystems actuators.

R–Fe-based alloys (R = rare earth) offer the possibility to develop very large magnetostrictions at room temperature. This is due to the highly aspherical 4f orbitals remaining oriented by the strong coupling between R and Fe moments. In order to exploit this property at reasonably low fields, it is essential to have low macroscopic anisotropy. A first route to low anisotropy is by using cubic compounds in which the second order anisotropy constants vanish. This is the case for the $RFe_2$ Laves phase compounds of which $TbFe_2$ (Terfenol), a ferrimagnet with $T_c = 710$ K, is probably the best known [4], having $\lambda_s = 1753 \times 10^{-6}$. The anisotropy can be further decreased by substitution of Tb by Dy in these compounds. This is due to Dy and Tb having opposite signs of the Steven's $\beta_J$ coefficient and thus their contributions to the fourth order anisotropy being of opposite sign. This leads to the magnetostriction, albeit less than in pure $TbFe_2$, being saturated in much lower fields. This is the case for the Terfenol-D material, the crystalline $(Tb_{0.27}Dy_{0.73})Fe_2$ compound, which has found many applications as high power actuators.

An alternative route to low macroscopic anisotropy is by using amorphous materials. In Fe-based amorphous alloys, both positive and negative exchange interactions exist [5], leading to magnetic frustration in the Fe sublattice. In a-YFe alloys, this results in a concentrated spin glass behaviour below room temperature. In a-RFe alloys, where R is a magnetic rare earth, the additional contributions of R–Fe exchange and local crystalline electric field interactions lead

† Permanent address: Cryogenic Laboratory, University of Hanoi, Vietnam.
‡ Corresponding author. Permanent address: Universitatea Babes-Bolyai, Romania.

0953-8984/00/367957+12$30.00  

to the formation of sperimagnetic structures [5]. The ordering temperatures are above room temperature ($T_c$ = 410 K for a-$Tb_{0.33}Fe_{0.66}$ [6, 7]). It is, however still rather low and is thus detrimental to large magnetostrictions being obtained in such materials at room temperature.

Actually, with a view to obtaining large magnetostrictions in the amorphous state, it is interesting to consider the equivalent a-RCo-based alloys. Although crystalline $RCo_2$ compounds order below 300 K as the Co is merely paramagnetic [8], the amorphous state stabilizes a moment on the Co sublattice due to band narrowing. These Co moments are strongly ferromagnetically coupled. A sperimagnetic structure occurs as in a-RFe alloys but the ordering temperature is now raised up to 600 K [7] for $Tb_{0.33}Co_{0.66}$. Recently we have studied a-$Tb_xCo_{1-x}$ and shown that large magnetostrictions of $b^{\gamma,2} = 300 \times 10^{-6}$ at 300 K are obtained for $x \sim 0.33$ [9, 10].

In general, however, R–Fe exchange energies are larger than the equivalent R–Co interaction energies [11]. This arises from the fact that the Fe moment is significantly larger than the Co one, while the R–T intersublattice exchange constant (T = transition metal) is approximately the same for T = Fe and Co. In addition, the T–T interactions tend to be stronger in (FeCo)- than in either Fe- or Co-based alloys [12]. This results in an increase of $T_c$ for a given R:T ratio. The stronger R–FeCo exchange energies should then lead to an enhancement of the R moment at room temperature and thus the magnetostriction in these amorphous alloys.

In the present paper, we have studied the influence of the Fe:Co ratio on the magnetization and magnetostriction of $(Tb_{0.27}Dy_{0.73})(Fe_{1-x}Co_x)_2$. We have chosen a fixed Tb:Dy ratio of 1:2.7, the same as that of Terfenol-D. The motivation for this was that, if the local environment in the amorphous state was the same as that in the crystalline one, a similar anisotropy reduction could potentially be obtained. We have shown elsewhere that such an anisotropy reduction can be obtained [13].

## 2. Experiment

The films were prepared by RF magnetron sputtering. The typical power during sputtering was 300 W and the Ar pressure was $10^{-2}$ mbar. A composite target was used allowing a wide range of alloys to be made in a controllable way without a large cost in materials. The target consisted of 18 segments of about 20°, of different elements (here Tb, Dy, Fe, Co). These were made by spark-cutting pure element discs. They were then assembled and stuck to a Cu sample holder using silver paint. It was verified by RBS and XEDS measurements that no Cu and Ag contamination had occurred. The target–substrate distance was 8 cm. The substrates were glass microscope cover-slips with a nominal thickness of 150 $\mu$m. Both target and sample holder were water cooled.

The ratio of the deposition rates of R = Tb, Dy to T = Fe, Co is 0.85. Thus, for the $(Tb_{0.27}Dy_{0.73})(Fe, Co)_2$ films made here, the Tb(Dy) and Fe(Co) concentrations could, in principle, be varied in steps of about 14% and 9%, respectively. The resulting composition, contamination and composition homogeneity were measured using XEDS and RBS analyses. The thicknesses were measured mechanically using an alpha-step and a DEKTAK profilometer and the sample mass was determined from the mass difference of the substrates before and after sputtering. The typical film thickness was 1.2 $\mu$m. X-ray $\theta$–$2\theta$ diffraction showed the samples to be amorphous.

Samples were annealed at 150 °C and 250 °C for 1 hour under a magnetic field of 2.2 T in order to relieve any stress induced during the sputtering process and to attempt to induce a well defined uniaxial in-plane anisotropy. Subsequent x-ray $\theta$–$2\theta$ diffraction showed no evidence for re-crystallization after annealing.

The magnetization measurements were carried out using a vibrating sample magnetometer in fields of up to 8 T from 4.2 K to 800 K.

The magnetostriction was measured using an optical deflectometer (resolution of $5 \times 10^{-8}$ rad), in which the bending of the substrate due to the magnetostriction in the film was measured. This allows the magnetoelastic coupling coefficient of the film, $b$, to be directly determined [14, 15] using:

$$b = \frac{\alpha}{L} \frac{h_s^2}{h_f} \frac{E_s}{6(1+\nu_s)} \tag{1}$$

where $\alpha$ is the deflection angle of the sample as a function of applied field, $L$ is the sample length, $E_s$ and $\nu_s$ are Young's modulus and the Poisson ratio for the substrate which are taken to be 72 GPa and 0.21 respectively. $h_s$, $h_f$ are the thicknesses of the substrate and film respectively. $L$ was typically of the order of 13 mm.

$b$ is proportional to the magnetostriction via Young's modulus and the Poisson ratio of the film. These cannot be reliably measured for thin films; however for comparison, we also give values of $\lambda$ calculated using

$$\lambda = \frac{b(1+\nu_f)}{E_f} \tag{2}$$

where $E_f$ and $\nu_f$ are Young's modulus and the Poisson ratio for the film, taken to be 80 GPa and 0.31 respectively. With the sample width of 3 mm, the error in this determination due to clamping is therefore less than 2% [16].

We measured two coefficients at saturation, $b_\parallel$ and $b_\perp$, which correspond to the applied field, always in the film plane, being respectively parallel and perpendicular to the sample length (i.e. the measurement direction). In addition, the perpendicular direction corresponds to the easy axis induced after field annealing. The intrinsic material dependent parameter, $b^{\gamma,2}$, (or $\lambda^{\gamma,2}$) is just the difference $b_\parallel - b_\perp$ (or $\lambda_\parallel - \lambda_\perp$).

## 3. Experimental results

### *3.1. Magnetization*

Figure 1 presents the hysteresis loops for several as-deposited $(Tb_{0.27}Dy_{0.73})(Fe_{1-x}Co_x)_2$ films at 4.2 K. In all samples, a large coercivity is observed and the magnetization does not completely saturate even at 8 T. Such large coercive fields are typical of amorphous RT alloys at low temperatures, where R is an non-S-state rare-earth. They are related to the strong local anisotropy of the R atoms and the random distribution of easy axes present in such sperimagnetic systems. The high-field susceptibility ($\chi_{hf}$) is also typical of sperimagnetic systems and is associated with the closing of the cone distribution of R moments as the field is increased [9].

The coercive fields reach their highest value of 3.4 T for $x = 0$. With increasing Co concentration, coercivity decreases rapidly down to about 0.5 T for $0.67 \leqslant x \leqslant 1.0$ (see figure 2(a)). $\chi_{hf}$ also decreases with increasing Co concentration, to a minimum at $x = 0.47$ and then slightly increases with further increasing $x$.

In all cases, $H_c$ also decreases with increasing temperature (see the inset in figure 2(a)) while $\chi_{hf}$ is strongly enhanced. This is due to the thermal decrease in the local anisotropy of the R atoms which is more rapid than that of the exchange field. In figure 2(b), we present $H_c$ at 300 K as a function of $x$. All the films are magnetically rather soft at room temperature and there is a maximum in $H_c$ at $x = 0.67$.

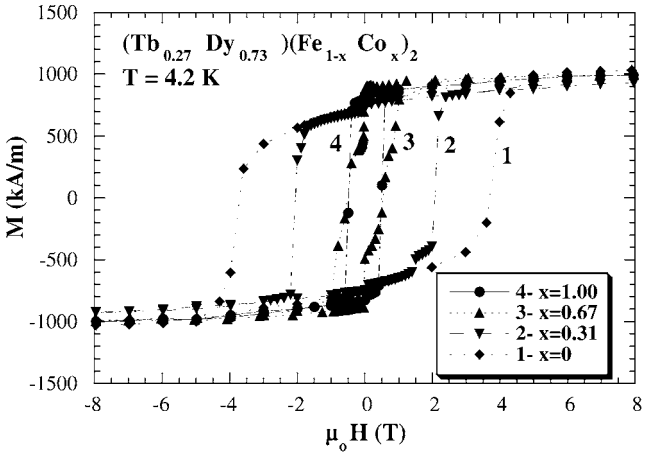


**Figure 1.** Hysteresis loops at 4.2 K for several $(Tb_{0.27}Dy_{0.73})(Fe_{1-x}Co_x)_2$ thin films.

The spontaneous magnetization values at 4.2 K and 300 K for the as-deposited $(Tb_{0.27}Dy_{0.73})(Fe_{1-x}Co_x)_2$ films extrapolated to zero field are shown in figure 3(a). At 4.2 K there is a maximum at $x = 0.47$ while at 300 K, within experimental errors, the magnetization is independent of the Co concentration. This is in contrast with the behaviour observed for the RT crystalline alloys (where R is a heavy rare earth) where $M_s$ shows a minimum in the middle of the composition range due to the enhancement of the 3d magnetic moment [17]. In the amorphous case, however, an increase in $M_{3d}$ will close the sperimagnetic cone. The maximum in $M_s$ at $x = 0.47$ reflects that, at low temperature, the enhancement of $M_{3d}$ is smaller than the associated increase in $\langle M_R \rangle$.

The thermal variation of the magnetization of these alloys is illustrated in figure 3(b) for $x = 0.67$. It is characterized by a decrease of magnetization with increasing temperature up to 420 K where there is a minimum in the measured magnetization. The magnetization then increases with increasing temperature. This thermal variation of the magnetization is completely reversible as measured by successive heating–cooling cycles between 425 K and 550 K, showing that the samples are still amorphous. This is also confirmed by subsequent x-ray diffraction. The observed minimum represents the compensation temperature and an ordering temperature higher than 550 K is expected for this alloy. This is consistent with values previously reported for the a-$RCo_2$ [7]. A compensation temperature is seen here for a-(Tb, Dy)$Fe_2$ unlike a-$TbFe_2$ due to the faster $M_{DyTb}(T)$ decrease compared to $M_{Tb}(T)$. Further heating–cooling cycles between (320–650 K) and (320–720 K) show a large hysteresis showing the importance of re-crystallization in this temperature range. However, this recrystallization masks the true ordering temperature of the amorphous phase.

Samples were annealed at temperatures between 425 K and 525 K in an applied magnetic field of 2.2 T. The field dependences of the magnetization before and after annealing are shown in figure 4 for $x = 1$. For the as-deposited samples (1), the magnetization reversal process is progressive and isotropic with a rather large coercive field. This property is often observed in sperimagnetic systems where domains of correlated moments are formed due to the competition between exchange interactions and random local anisotropy. These domains, termed Imry and Ma domains [18, 19], are oriented more or less at random in zero field but can be re-oriented under applied field.

After annealing, there are a number of clear differences in the magnetization process. Firstly, the coercive field is strongly reduced. Figure 2(b) shows the coercive field as a function

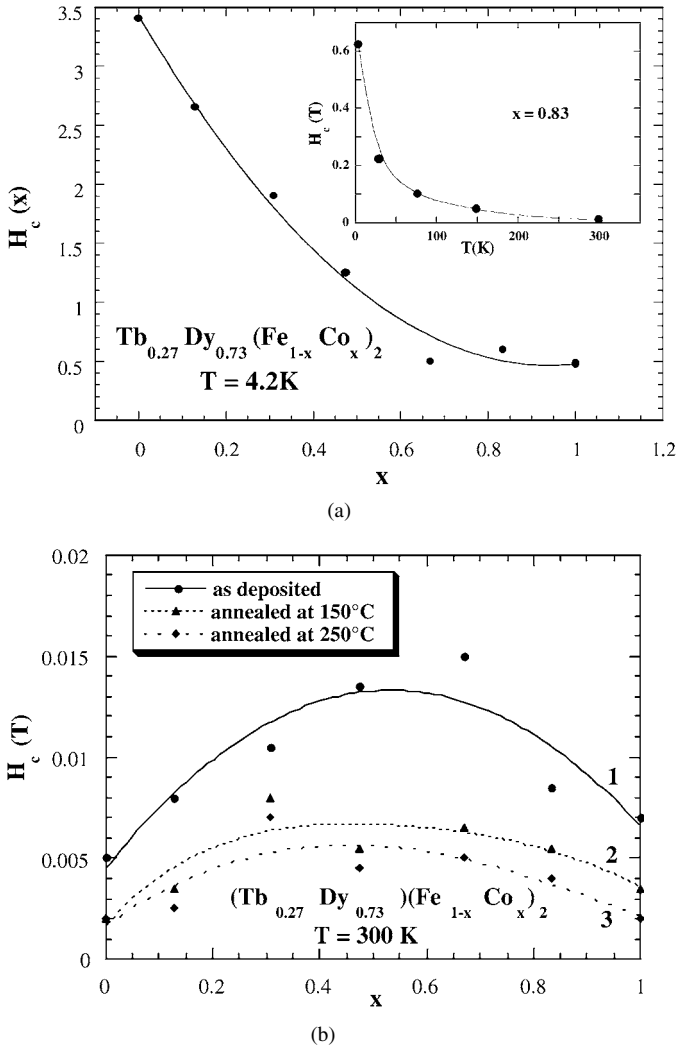


**Figure 2.** (a) Coercive field $H_c$ as a function of Co concentration at 4.2 K. The inset shows the temperature dependence of $H_c$ for $x = 0.83$. (b) Coercive field $H_c$ as a function of Co concentration at 300 K: (1) the as-deposited films, (2) after annealing at 150 °C and (3) after annealing at 250 °C.

of composition before and after annealing. After annealing at 525 K, $H_c$ is less than 2 mT for all compositions with only a slight maximum around the middle of the composition range. Secondly, for this sample, there is now a well defined easy axis with an increased low field susceptibility. These properties are characteristic of systems which show uniaxial anisotropy. That such an anisotropy is induced by annealing suggests that a process of single ion directional ordering [20] has occurred, in which there is a local reorientation of the Tb easy axes along the field direction. The composition dependence of this uniaxial anisotropy is, however, more complex and will be discussed further in connection with the magnetostriction data. The field annealing also causes a reduction in $\chi_{hf}$, indicating that the cone distribution of the Tb moments is somewhat closed.

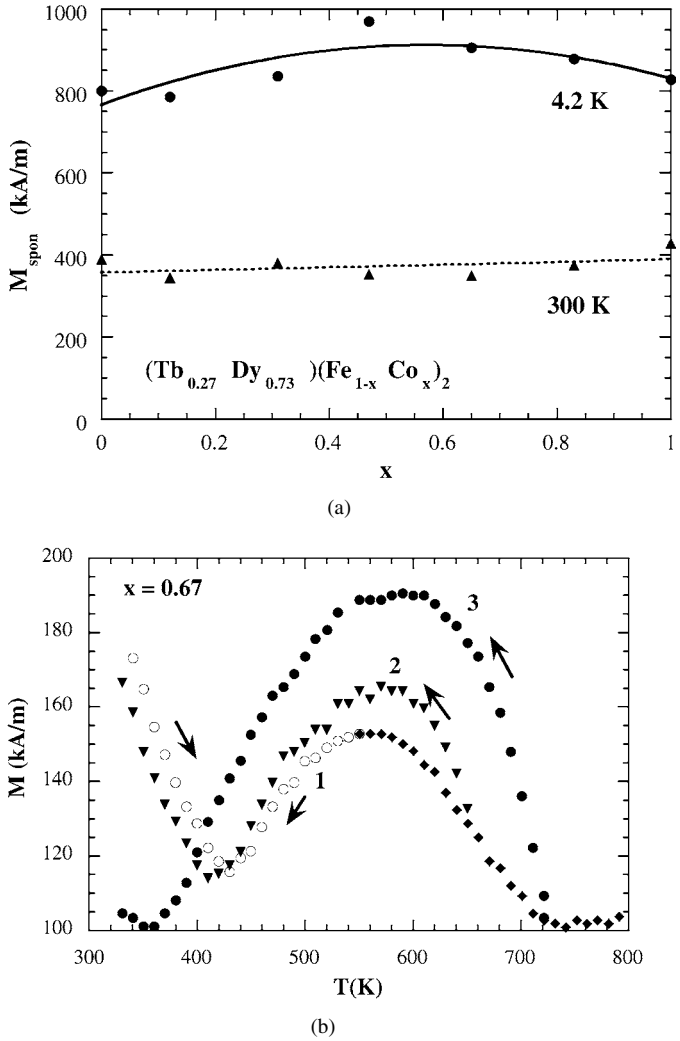


**Figure 3.** (a) Variation of spontaneous magnetization as a function of $x$ at 4.2 K and 300 K for $(Tb_{0.27}Dy_{0.73})(Fe_{1-x}Co_x)_2$ thin films. (b) Thermal variation of the magnetization for $(Tb_{0.27}Dy_{0.73})(Fe_{1-x}Co_x)_2$ thin films for different heating–cooling cycles: (○) reversible part (1); filled marks—irreversible parts (2 and 3): (▲) 650 K–320 K and (●) 720 K–320 K.

### *3.2. Magnetostriction*

In general, the comparison of the magnetoelastic coupling coefficient $b_\parallel$ and $b_\perp$ (see section 2) indicates clearly the anisotropy state of the sample. If the zero field state is fully isotropic, then $b_\parallel = -2b_\perp$ and if it is isotropic in the plane, then $b_\parallel = -b_\perp$ [21]. For a well defined in-plane, uniaxial system, magnetization reversal under a field, $H$, applied along the easy axis, occurs by 180° domain wall displacement. Neglecting domain wall contributions, no magnetostriction is associated with this process. Thus $b_\perp$ should be zero and $b_\parallel = b^{\gamma,2}$.

The magnetostriction results are summarized in figure 6(a) across the entire composition range. It is clear that the annealing affects very differently the Fe-rich alloys compared to the Co-rich ones. For the Co-rich alloys, $b_\parallel$ increases significantly after annealing while

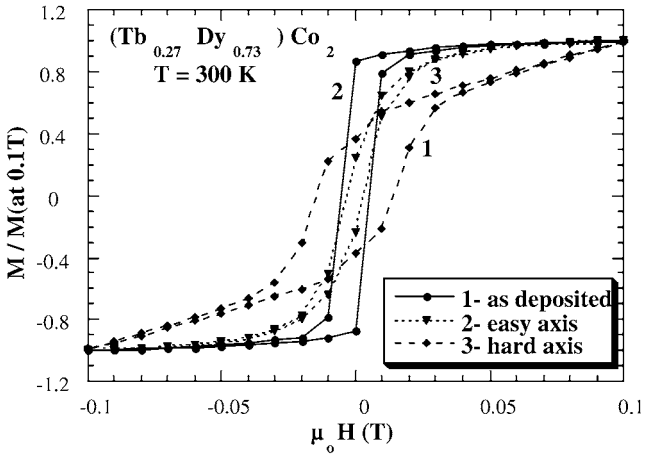


**Figure 4.** Hysteresis loops for the $(Tb_{0.27}Dy_{0.73})Co_2$ (1) as-deposited film and (2) after annealing—along induced easy axis and (3) hard axis.

$b^{\gamma,2}$ remains virtually unchanged. For the Fe-rich alloys, we see the opposite effect in that $b^{\gamma,2}$ increases significantly after annealing while $b_{\parallel}$ remains virtually unchanged. The largest magnetostriction of $\lambda^{\gamma,2} = 480 \times 10^{-6}$ (in 1.8 T external field) and $\lambda_{\parallel} = 250 \times 10^{-6}$ (obtained in very low applied magnetic fields of 0.06 T) is found in the middle of the composition range at $x = 0.47$. These differences in anisotropy are also reflected in figure 6(b) which shows the ratio of $b_{\parallel}$ to $b_{\perp}$ before and after annealing. Figure 5 shows this effect of annealing on the magnetostriction for two alloys with $x = 0.83$ and $x = 0$. For $x = 0.83$ (see figure 5(a)), we see that annealing increases the ratio of $b_{\parallel}$ to $b_{\perp}$ while $b^{\gamma,2}$ remains roughly constant. This is due to the creation of an in-plane uniaxial anisotropy as seen from magnetization measurements. In addition we see that this anisotropy is completely defined after annealing at 425 K and is accompanied by a reduction in the saturation field. Subsequent annealing at 525 K simply further reduces the saturation field. For the $x = 0$ sample (see figure 5(b)), we see a different behaviour. Before annealing, the approach to saturation is rather slow and the ratio of $b_{\parallel}$ to $b_{\perp}$ indicates an initial anisotropy. After annealing, the saturation field is reduced and this initial anisotropy is destroyed, leaving the sample almost isotropic. However, $b^{\gamma,2}$ (measured at 1.8 T) actually increases after annealing.

## 4. Discussion

The magnetic properties of these alloys are rather complex but it is important to attempt to understand them in order to better optimize the magnetostrictive properties of such alloys with respect to potential applications. One of the main differences between the magnetic properties of amorphous $RT_2$ alloys and their crystalline counterparts is the sperimagnetic distribution of R and Fe moments in the amorphous case [13]. This sperimagnetic structure arises from the competition between exchange interactions and random local anisotropy and leads to the formation of domains of correlated moments known as Imry and Ma domains [18]. These domains are oriented more or less at random in zero field and the macroscopic anisotropy energy, which determines the coercive field, is an average of the random local anisotropy over the volume of each domain [22]. This non-collinear magentic structure can also be described in terms of a sperimagnetic cone, within which the Tb and Dy moments lie. The angle of the

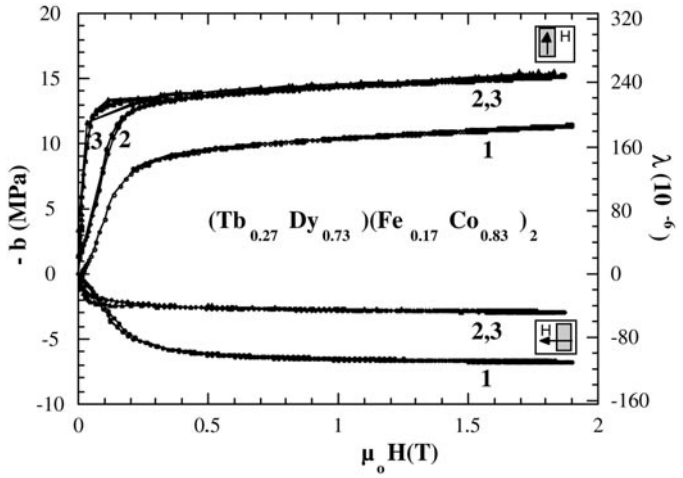


(a)

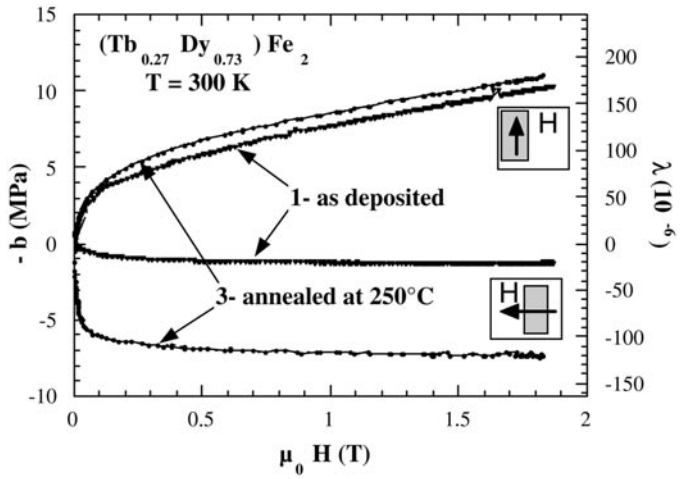


(b)

**Figure 5.** (a) Magnetostriction for $x = 0.83$ (1) as-deposited film, (2) annealing at 150 °C and (3) 250 °C. (b) Magnetostriction for $x = 0$ (1) as-deposited film and (3) 250 °C.

cone is determined by the competition of the local anisotropy to the exchange energy. The magnetostriction is very sensitive to changes in the R sublattice. At room temperature, the maximum in magnetostriction at $x = 0.47$ indicates that the R sublattice undergoes some changes as a function of $x$. This cannot be seen in the magnetization as a function of $x$. We will now discuss this effect.

Assuming that the R moments have the same value as in the crystalline Laves phase, we can estimate the magnetostriction of a sperimagnetic system with respect to a collinear ferrimagnetic one using [9]:

$$b^{\gamma,2} = \tfrac{3}{2} b_{int}^{\gamma 2} (\langle \alpha_z^2 \rangle - \tfrac{1}{3})$$

where $\alpha_z$ is the direction cosine for each rare-earth moment with respect to the field direction and $b_{int}^{\gamma 2}$ is an intrinsic magnetoelastic coupling coefficient (i.e. that of the collinear ferrimagnet).

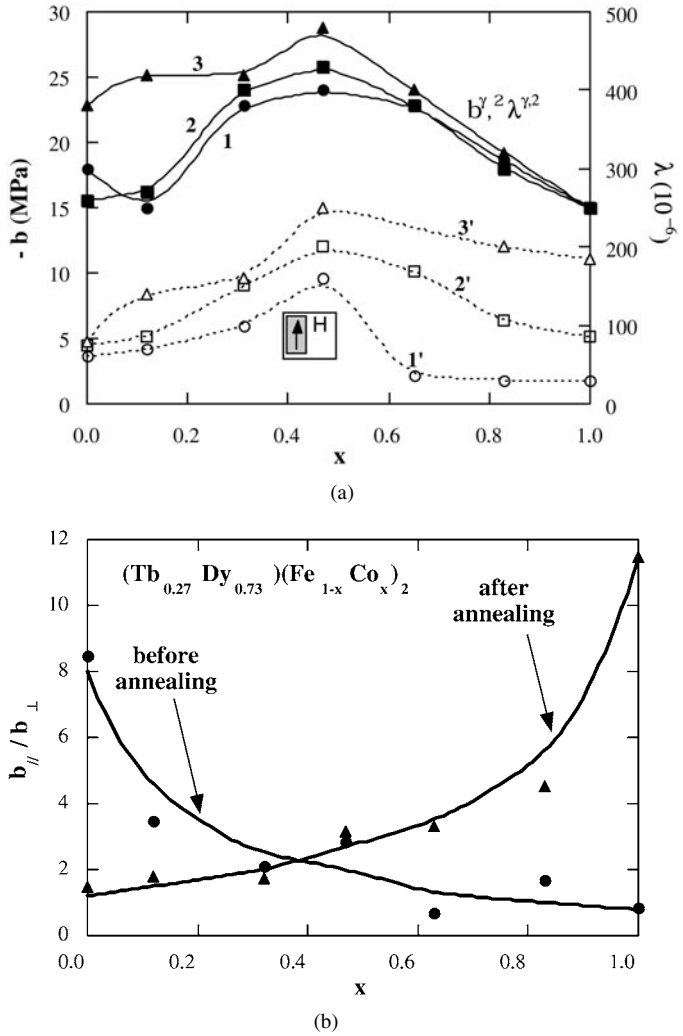


**Figure 6.** (a) Magnetostriction $\lambda^{\gamma,2}$ (1.8 T) and $\lambda_\parallel$ (0.06 T) for the $(Tb_{0.27}Dy_{0.73})(Fe_{1-x}Co_x)_2$ as-deposited thin films (1, 1′), films annealed at 150 °C (2, 2′) and at 250 °C (3, 3′). (b) Ratio $b_\parallel/b_\perp$ as a function of $x$ before and after annealing.

Here, we take $b_{int}^{\gamma 2} = 127$ MPa, the room temperature value of $b^{\gamma,2}$ in isotropic polycrystalline crystalline $(Tb_{0.27}Dy_{0.73})Fe_2$ [23]. Assuming a uniform probability distribution of easy axes within a cone, and that the intrinsic value of $R$ does not vary, we can deduce the characteristic sperimagnetic cone angle, $\theta$ as a function of $x$. Here, this gives values of between 48 and 53° which are typical of those reported in the literature [5, 24]. This variation in $\theta$ implies that there is a variation in the average (Tb, Dy) moment as a function of $x$. Using $M_{(TbDy)} = 7.27\,\mu_B$, the room temperature value in $(Tb_{0.27}Dy_{0.73})Fe_2$ [4], we can deduce $\langle M_{TbDy}\rangle = M_{(TbDy)}\langle\alpha_2\rangle$, as a function of $x$, and this is plotted in figure 7. From the measured magnetization data, we can now deduce $M_{3d}$ as a function of $x$ (figure 7). The values thus determined are in good agreement with those found for $M_{3d}$ in 'pure' a-$TbCo_2$ and a-$TbFe_2$ alloys [6] at room temperature. This indicates that there is an enhancement in $M_{3d}$ for the substituted a-$R(Fe, Co)_2$ alloys and a maximum is reached for $x = 0.47$ where there is sufficient Co to ensure good ferromagnetic

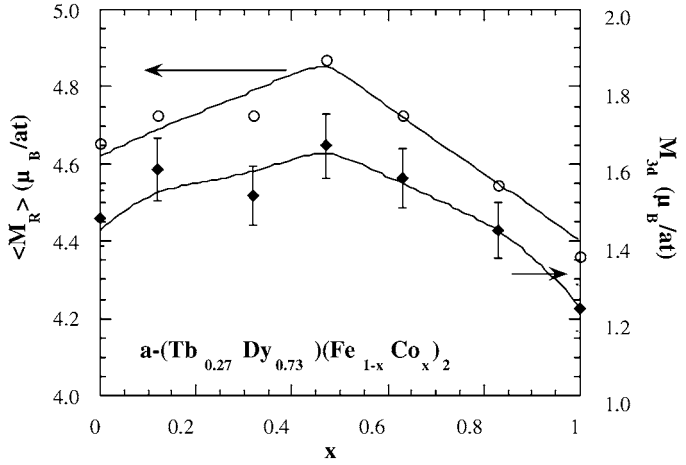


**Figure 7.** Calculated variation of $\langle M_R \rangle$ and $M_{3d}$ from magnetostriction data as a function of $x$ (see text).

T–T coupling as well as sufficient Fe giving the larger magnetic moment. We have, of course, neglected the variation in ordering temperature and hence intrinsic R moment value at room temperature associated with such an enhancement of the T–T interactions. However, this simple analysis illustrates the importance of considering the influence of the sperimagnetic structure on the magnetostriction and the magnetic properties of such alloys.

An intriguing aspect in this study is the variation of the anisotropy state as a function of T composition, before and after annealing. The comparison of $b_\parallel$ to $b_\perp$ is a useful tool for understanding the role of Co in these alloys (figure 6(b)). For the Fe-rich alloys before annealing, $b_\parallel/b_\perp$ is large indicating a well defined initial in-plane anisotropy. However, the magnetization measurements show that there is no in-plane anisotropy. After annealing, $b_\parallel/b_\perp \approx 2$ suggesting that the zero field magnetization state now is fully isotropic. These two elements together imply anisotropy in the as-deposited state and that this is destroyed in the annealing process. Note also that the as-deposited material is not completely saturated at 1.8 T, while after annealing saturation is achieved at around 1 T. This leads to the measured increase in $(b_\parallel - b_\perp)$ at 1.8 T after annealing.

For the as-deposited Co-rich alloys, $b_\parallel/b_\perp \approx -1$, i.e. the film has isotropic in-plane magnetization. After annealing at 250 °C, $b_\parallel/b_\perp$ varies from 4 to 10 (figure 6(b)), showing that a well defined in-plane anisotropy direction has been induced. The origin of the differing anisotropies in the as-deposited state is unknown, and further studies should be made. It has often been noted that Fe-based RT compounds have a different anisotropy state compared to their Co-based counterpart.

The annealing process, although efficient, still remains little understood. While we invoke a single ion anisotropy as being at the heart of the process, it is more difficult to explain why the results are so different for Co-based and Fe-based alloys.

We suggest two possible, but not unrelated, reasons for this difference. During the annealing process, it is the local internal field that is responsible for the reorientation of the R moments. The strongly ferromagnetically coupled Co sublattice is well ordered and acts to orient the R sublattice in one direction, giving rise to the observed uniaxial anisotropy. However, the Fe sublattice is magnetically sperimagnetic and is relatively unchanged by a small external applied field. The external field is present to remove magnetostatically induced

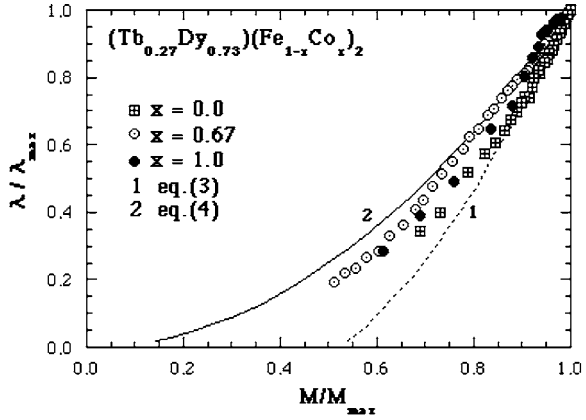


**Figure 8.** Experimental and theoretical relations between magnetostriction and magnetization (see text) for amorphous $(Tb_{0.27}Dy_{0.73})(Fe_{1-x}Co_x)_2$ thin films.

domains. Therefore during the annealing process of Fe-based alloys the R atoms see a randomly oriented local magnetic field while the Co-based alloys see a homogenoeus magnetic field.

The second possibility is that $T_c$ increases going from Fe to Co. At the annealing temperature, the Fe-based alloys are no longer magnetic while the Co-based ones are. This variation is again due to the sperimagnetic nature of the amorphous Fe sublattice. Further work must be carried out to clarify this area as it is important for a number of applications of such materials.

We can further illustrate this variation in anisotropy by associating the field dependence of the magnetostriction with different types of magnetization processes. For a system of randomly oriented spin and random distribution of the domain walls, the magnetization process takes place in two steps [25]. First, the motion of 180° domain walls leads to a magnetization of $M_0$ without any contribution to the magnetostriction. In the second step, the spins rotate into the direction of the applied magnetic field leading to the change of both magnetization and magnetostriction.

For a uniaxial system with random distribution of easy axis, the value $M_0$ obtained after complete wall motion is equal to $M_{max}/2$. The relation between magnetostriction and magnetization is then given as [1]:

$$\lambda(H)/\lambda_{max} = [2M(H)/M_{max} - 1]^{3/2}. \tag{3}$$

Alternatively, in the case where a unique easy axis exists, under the effect of the field, when the magnetization rotates out of the easy axis, the magnetostriction is given by [25]

$$\lambda(H)/\lambda_{max} = [M(H)/M_{max}]^2. \tag{4}$$

The experimental values of $\lambda/\lambda_{max}$ are plotted as a function of $M/M_{max}$ in figure 8. The experimental data for the (Tb, Dy)Fe film are rather well described by equation (3). With increasing Co concentration, the $\lambda/\lambda_{max}$ versus $M/M_{max}$ curves shift towards the line described by equation (4). This further confirms that the Co substitution is advantageous to the creation of a well defined easy axis in this system.

## 5. Concluding remarks

In conclusion, we would like to point out that larger magnetostrictions are obtained in amorphous (Tb, Dy)(Fe, Co) films as compared to their parent amorphous films of either

(Tb, Dy)Fe or (Tb, Dy)Co. This has been explained in terms of an increase in the ferromagnetic coupling strength within the (Fe, Co) sublattice [12]. In addition, a well defined uniaxial anisotropy can be induced by magnetic field annealing for the Co-rich films.

It is well known that the substitution of Dy for Tb gives rise to an increase in the magnetostriction at low magnetic fields, through the reduction of the saturation field. However, this is also accompanied by a reduction in the saturation magnetostriction. In this study we have shown that Co substitution, coupled with the effects of annealing, result in an enhancement of both the low-field and the saturation magnetostriction. Thus we can expect a further enhancement of the magnetostriction in these alloys by increasing the Tb concentration. Indeed, we have obtained a giant magnetostriction of $\lambda^{\gamma,2} = 1020 \times 10^{-6}$ at 1.8 T with $\lambda_{\|} = 585 \times 10^{-6}$ at 0.1 T in amorphous $Tb(Fe_{0.55}Co_{0.45})_2$ [13].

## Acknowledgments

The authors thank Dr E du Trémolet de Lacheisserie for helpful discussions. The work of N H Duc is supported by the CNRS within the PRI-PED scheme. This work was carried out as part of the EC funded 'Magnifit' project (contract number BRE2-0536).

## References

[1] Honda T, Arai K I and Yamaguchi M 1994 *J. Appl. Phys.* **76** 6994
[2] Quandt E 1994 *J. Appl. Phys.* **75** 5653
[3] Speliotis A, Kalogirou O, Vouroutzis N and Niarchos D 1998 *J. Magn. Magn. Mater.* **187** 17
[4] Clark A E 1980 *Ferromagnetic Materials* vol 1, ed E P Wohlfarth (Amsterdam: North-Holland) p 531.
[5] Coey J M D, Givord D, Liénard A and Rebouillat J P 1981 *J. Phys. F: Met. Phys.* **11** 2707
[6] Hansen P, Clausen C, Much G, Rosenkranz M and Witter K 1989 *J. Appl. Phys.* **66** 756
[7] Lee K and Heiman N 1973 *AIP Conf. Proc. 18, section 7, Amorphous Magnetic Materials* pp 108–9
[8] Lemaire R 1966 *Cobalt* **33** 201–11
[9] Betz J 1997 Giant magnetostriction of thin films and magnetostrictive microactuators for integrated technologies *Physics Thesis* University Joseph Fourier of Grenoble
[10] Betz J, Mackay K and Givord D 1999 *J. Magn. Magn. Mater.* **207** 180
[11] Liu J P, de Boer E R, de Châtel P F, Coehoorn R and Buschow K H J 1994 *J. Magn. Magn. Mater.* **134** 159
[12] Gavigan J P, Givord D, Li H S and Voiron J 1988 *Physica* B **149** 345
[13] Duc N H, Mackay K, Betz J and Givord D 1996 *J. Appl. Phys.* **79** 973
[14] Trémolet de Lacheisserie E and Peuzin J C 1994 *J. Magn. Magn. Mater.* **136** 189
[15] Betz J, du Trémolet de Lacheisserie E and Baczewski L T 1996 *Appl. Phys. Lett.* **68** 132
[16] Iannotti V and Lanotte L 1999 *J. Magn. Magn. Mater.* **202** 191
[17] Pourarian F, Wallace W E and Malik S K 1981 *J. Magn. Magn. Mater.* **25** 299
[18] Imry Y and Ma S 1975 *Phys. Rev. Lett.* **35** 1399
[19] Boucher B, Liénard A, Rebouillat J P and Schweizer J 1979 *J. Phys. F: Met. Phys.* **9** 1421
Boucher B, Liénard A, Rebouillat J P and Schweizer J 1979 *J. Phys. F: Met. Phys.* **9** 1433
[20] Néel L 1953 *C. R Acad. Sci. Paris.* **237** 1468
Néel L 1954 *J. Phys. Radium* **15** 225
[21] Schatz F, Hirscher M, Schnell M, Flik G and Kronmüller H 1994 *J. Appl. Phys.* **76** 5380
[22] Alben R, Bundrick J I and Cargill G S 1978 Magnetic structures *Metallic Glasses* (Metals Park, OH: American Society for Metals) ch 12
[23] The values given in [4] are for somewhat textured samples. Here we calculate $b^{\gamma,2}$ for an isotropic polycrystalline sample of $Tb_{0.27}Dy_{0.73}Fe_2$, using single crystal data. $b^{\gamma,2} = 3G\lambda_s$ with $1/(2G) = 2/5s\gamma + 3/5s^{\varepsilon}$ and $\lambda_s = 0.6\lambda_{111}$.
du Trémolet de Lacheisserie E private communication
[24] Hansen P 1991 *Ferromagnetic Materials* vol 6, ed K H J Buschow (Amsterdam: North-Holland) p 289
[25] Chikazumi S 1964 *Physics of Magnetism* (New York: Wiley)